Journal Pre-proof

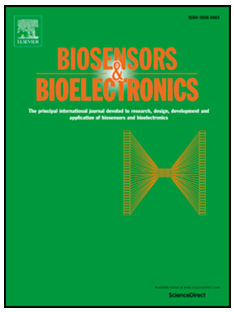

Real-time point-of-care total protein measurement with a miniaturized optoelectronic biosensor and fast fluorescence-based assay

Fariah Mahzabeen, Ophir Vermesh, Jelena Levi, Marilyn Tan, Israt S. Alam, Sanjiv S. Gambhir, James S. Harris

PII: S0956-5663(20)30809-5

DOI: https://doi.org/10.1016/j.bios.2020.112823

Reference: BIOS 112823

To appear in: *Biosensors and Bioelectronics*

Received Date: 16 December 2019

Revised Date: 10 November 2020

Accepted Date: 12 November 2020

Please cite this article as: Mahzabeen, F., Vermesh, O., Levi, J., Tan, M., Alam, I.S., Gambhir, S.S., Harris, J.S., Real-time point-of-care total protein measurement with a miniaturized optoelectronic biosensor and fast fluorescence-based assay, *Biosensors and Bioelectronics* (2020), doi: https://doi.org/10.1016/j.bios.2020.112823.

Credit Author Statement

Fariah Mahzabeen: Conceptualization, Methodology, Investigation, Formal Analysis, Writing – Original Draft. **Ophir Vermesh**: Conceptualization, Methodology, Investigation, Formal Analysis, Validation, Data Curation, Writing – Original Draft, Writing – Review & Editing, Supervision, Project Administration. **Jelena Levi**: Methodology, Investigation, Resources, Writing – Review & Editing. Marilyn Tan: Resources, Writing – Review & Editing. **Israt Alam:** Investigation, Visualization, Writing – Review & Editing. **Carmel Chan**: Visualization, Writing – Review & Editing. **Sam Gambhir**: Conceptualization, Supervision, Project administration, Resources, Funding acquisition, Writing – Review & Editing. **James Harris**: Conceptualization, Supervision, Project administration, Resources, Funding acquisition, Writing – Review & Editing.

Title: Real-Time Point-of-Care Total Protein Measurement with a Miniaturized Optoelectronic Biosensor and Fast Fluorescence-Based Assay

Authors: *Fariah Mahzabeen[1,†], Ophir Vermesh[2,3,†,*], Jelena Levi[2,3], Marilyn Tan[4], Israt S. Alam[2,3], Sanjiv S. Gambhir[2,3,5,6,*], James S. Harris[1,*]*

Affiliations:

[1]*Department of Electrical Engineering, Stanford University, Stanford, CA, 94305, USA*

[2]*Department of Radiology, Stanford University, Stanford, CA, 94305, USA*

[3]*Molecular Imaging Program at Stanford, Stanford University, Stanford, CA 94305*

[4]*Department of Medicine, Stanford University, Stanford, CA 94305*

[5]*Department of Bioengineering, Stanford University, Stanford, CA 94305*

[6]*Stanford Bio-X, Stanford University, Stanford, CA 94305*

† Authors contributed equally

** To whom correspondence should be addressed:*

Sanjiv Sam Gambhir, MD, PhD; Chair, Department of Radiology, Director, Molecular Imaging Program at Stanford (MIPS); Professor, Department of Radiology, Stanford University, The James H Clark Center, 318 Campus Drive, East Wing 1st Floor, Stanford, CA 94305; Phone: 650-725-2309; Email: sgambhir@stanford.edu

Keywords: Sensor, point-of-care, real-time, PIFE, VCSEL, nephropathy

Abstract: Measurement of total protein in urine is key to monitoring kidney health in diabetes. However, most total protein assays are performed using large, expensive laboratory chemistry analyzers that are not amenable to point-of-care analysis or home monitoring and cannot provide real-time readouts. We developed a miniaturized optoelectronic biosensor using a vertical cavity surface-emitting laser (VCSEL), coupled with a fast protein assay based on protein-induced fluorescence enhancement (PIFE), that can dynamically measure protein concentrations in protein-spiked buffer, serum, and urine in seconds with excellent sensitivity (urine LOD=0.0004

g/dL, LOQ=0.0013 g/dL) and over a broad range of physiologically relevant concentrations. Comparison with gold standard clinical assays and standard fluorimetry tools showed that the sensor can accurately and reliably quantitate total protein in clinical urine samples from patients with diabetes. Our VCSEL biosensor offers a portable, low-cost, easy-to-use format for sensitive, accurate, and real-time total protein measurements from small biofluid volumes.

Introduction

Diabetes mellitus affects 30 million Americans and is the most common cause of renal failure worldwide[1, 2]. Nephropathy occurs in about 20 – 40% of patients with diabetes, with a large number of patients progressing to end-stage renal disease (ESRD) and cardiovascular disease (CVD)[1]. Microalbuminuria (MA), the presence of serum albumin at low levels (30-300 mg/L) in urine, is a well-established marker of increased renal and CVD risk that is present in up to 40% of patients with diabetes[3,4], and in 5-7% of healthy individuals who are at increased risk of CVD as well[36-39]. Even a small increase in urine albumin in these patients is associated with subsequent development of clinical nephropathy. However, patients with diabetes are typically tested for MA only once a year[5] in the clinic and do not have access to a method for accurate and routine monitoring of their kidney health at home. Regular screening for microalbuminuria could enable early detection of renal disease when it is still reversible, reducing both mortality and treatment cost in those affected[6,7].

The gold-standard microalbumin tests, which include turbidimetric and nephelometric immunoassays[8, 9], are performed in a clinical lab and are not cost-effective due to their reliance on antibodies[9]. More rapid, low-cost alternatives that measure urine total protein as a surrogate for urine albumin have been investigated[10-12]. Established quantitative protein assays employ either: 1) a colorimetric dye (e.g. Coomassie Blue, Pyrogallol Red) that changes absorbance upon binding to proteins[13,14]; 2) a redox reaction of copper ions with peptide bonds, leading to a color change (BCA, Lowry assays)[14-17]; or 3) turbidimetric assays using trichloroacetic acid, sulfosalicylic acid, benzethonium or benzalkonium chloride[18]. However, these methods cannot provide real-time measurements, and require expensive, bulky instrumentation for readout and highly trained personnel to process and interpret the data. Such complications preclude their use

at home or at the point of care. While the urine dipstick is a simple, inexpensive, and fast colorimetric method, it is not quantitative nor sufficiently sensitive, and is thus prone to false positive or negative results [17].

Herein, we introduce a miniaturized fluorescence-based sensor that is capable of real-time, sensitive measurement of total protein from a biological sample in a single step. The device - consisting of a vertical-cavity surface-emitting laser (VCSEL), a PIN photodetector, and optical filters integrated on-chip - harnesses the protein-induced fluorescence enhancement (PIFE) of a near-infrared cyanine dye in the presence of sample protein. Given their small size, modularity and minimal threshold power requirements (<1.5 mW)[19], VCSELs can be manufactured in arrays at high yield and low cost[19,20], provide superior wavelength stability (~5-fold less sensitive to temperature variations), and consume less power compared with light-emitting diodes (LEDs) or conventional edge-emitting lasers. They are thus an ideal source for wireless point-of-care sensors[20]. A key benefit for fluorescence-based detection is a narrow spectral linewidth (< 0.2nm in single mode) [20], which produces sharp excitation of the desired fluorescent probe and maximizes the spectral separation from the emission peak for more efficient spectral filtration, thereby improving fluorescence sensitivity and resolution. VCSELs also produce a low divergence output beam, facilitating coupling with a small sample while minimizing crosstalk with the photodector[20].

Previous work using VCSELs for analyte detection employed external off-chip components (PIN or CMOS photodetectors) or large benchtop fluorimeters[21-23], which limited their portability. More recently, we demonstrated monolithic integration of a VCSEL laser and a PIN detector on a single GaAs substrate[24]. Although this monolithic design offered extreme miniaturization prospects, its performance was limited by interlayer and lateral optical crosstalk

(spontaneous emission) between the laser and photodetector[25]. To overcome this limitation while still maintaining a small device footprint, separate VCSEL and detector components were discretely integrated in the current work into a packaged sensor.

In previous literature, VCSEL biosensors (e.g. for dengue virus and aflatoxin detection) have been described that incorporate multi-step heterogeneous immunoassays[22], which require surface functionalization with antibodies as well as multiple incubation and washing steps, rendering them laborious and time-consuming. Our biosensor measures the proportionate fluorescence increase that occurs upon interaction of a protein with free cyanine dye (Cy5.5) in a simple one-step homogeneous assay (**Fig. 1a**). The PIFE effect results from the non-covalent interaction between a protein and a cyanine dye, which sterically inhibits formation of the fluorescently inactive *cis* isomer and stabilizes the *trans* conformation in the excited state, resulting in a higher fluorescence quantum yield and a longer excited-state lifetime[26, 27] (**Fig. 1b, c**). For example, Cy3 has been shown to undergo ~2.4-fold increase in quantum yield and a 10-fold increase in fluorescence lifetime upon binding to protein[28]. While the PIFE effect has been harnessed in other studies (e.g. monitoring DNA dynamics in protein conformation or nucleic acid interactions) [29-33], we show that the instantaneous increase in fluorescence intensity that occurs upon mixing a protein-containing sample with a cyanine dye enables *real-time* protein sensing with a miniaturized sensor. To our knowledge, this is the first demonstration of a VCSEL sensor coupled with a PIFE assay for real-time sample analysis of total protein concentration.

In this paper, we first describe our protein sensor design and operation. We then characterize the sensor's signal response using buffer spiked with proteins and human serum, and compare the sensor's performance to that of benchtop fluorimeters. Finally, we test the accuracy

of our sensor for measuring total protein concentrations by analyzing clinical urine samples from patients with diabetes, and compare our results with values obtained using a gold standard clinical lab method.

Sensor Design. The VCSEL biosensor is designed to excite and record fluorescence in the near infrared (NIR) region. Our prototype consists of two commercially available 675 nm VCSELs (second laser for redundancy) and a custom-fabricated PIN GaAs detector wire bonded on a TO-5 (Transitor Outline, Case Style 5) metal can package. A PIN detector was chosen for its lower power consumption, smaller size, and much simpler and cheaper integration than photomultiplier tube (PMT) or complementary metal-oxide-semiconductor (CMOS) detectors. The VCSELs are placed on a quartz spacer for electrical isolation and spatial separation from the detector, reducing cross-talk, which is further mitigated with a black Ti/Au baffle (**Fig. 2a**). Placing the VCSEL and detector in a coplanar arrangement decreases background interference and improves limit of detection over an arrangement in which the excitation light is incident on the detector. On top of the detector sits an integrated dielectric notch filter combined with a hybrid bonded fluorescence emission filter for maximum rejection of excitation light. The package height and diameter are both 9 mm, excluding the leads (**Fig. 2a**). The package sidewalls are painted black to reduce stray light reflection. Integration is complete with mounting of an anti-reflective collimation lens (NA=0.55, Thorlabs, Newton, NJ). The packaged sensor is then placed in a specially designed cage (~1.5 inches) (**Fig. 2b**) built with black metal optical mounts (Thorlabs, Newton, NJ). The cage holds a sample well ~1 mm above the sensor, ensuring maximum coupling of fluorescence excitation and emission beams. Furthermore, the cage acts as a shield to external light interference, significantly reducing variability. The integrated device is connected

to external electronics, including a lock-in amplifier, signal generator, and computer (**Fig. 2c**). These electronic components are commercially available in miniaturized form and can potentially be integrated with the sensor within a <3-inch form factor to create a portable handheld device.

Sensor Operation. For sensor measurement of a protein-containing biofluid, a few microliters of sample are first diluted in buffer (~100-fold for serum and 10-fold for urine) to a total volume of ~150 µL, a volume chosen because it fits comfortably within the 300 µL sample well of the VCSEL biosensor. One microliter of Cy5.5 dye solution (1mg/mL) is then pipetted to the sample well. Alternatively, the sample solution can be premixed with dye and then transferred to the sample well. Sample fluorescence from VCSEL laser excitation is captured by the on-chip detector, and the photocurrent signal is amplified and then filtered by a lock-in amplifier and routed to a computer for visualization.

Methods

Study Design. The objective of this study was to design and implement a fully-integrated, miniaturized fluorimetric sensor for point-of-care and at-home monitoring, capable of rapidly and reliably detecting protein levels in patient serum and urine samples. Incorporation of a VCSEL laser afforded the requisite device miniaturization, while harnessing the PIFE effect afforded fast measurement speeds. We conducted controlled laboratory experiments to assess the response time of the sensor for detecting proteins in buffer, and tested the sensitivity, dynamic range, and linearity of the sensor in buffer as well as in human blood and urine samples. We also compared the performance of our sensor with that of benchtop fluorimetry. In all studies, protein

concentrations were tested in triplicate. Finally, we performed a study on urine samples from 14 patients with diabetes (each patient sample run in triplicate) to determine the accuracy of the sensor by comparing with a gold standard method.

Protein-spiked buffer solutions. A protein cocktail containing 0.1% human serum albumin (HSA) and 0.1% immunoglobulin G (IgG) (10:7 ratio) in phosphate-buffered saline (PBS) was prepared to simulate the relative protein composition in plasma. The cocktail was serially added in two-fold increments, starting with 4 µL, to PBS in separate microcentrifuge tubes (149 µl total volume). One microliter of a 1 mg/mL Cy5.5 dye solution in dimethylformamide (DMF) was added to each tube and the tubes were vortexed for 3s to ensure uniform mixing.

Serum-spiked buffer solutions. Pooled human serum (obtained from the Stanford Blood Bank, Stanford, CA) was serially spiked in two-fold increments, starting at 0.5 µL, to PBS in separate microcentrifuge tubes (149 µL total volume) to create solutions with a wide range of serum protein concentrations (0.003 - 0.41 g/dL). One microliter of 1 mg/mL Cy5.5 dye solution was added to each tube and mixed. Protein concentrations of the serum-spiked samples were measured using the Pierce BCA Protein Assay Kit (Thermofisher, Walthum, MA) according to the manufacturer's protocol and then tested with the VCSEL biosensor to assess the accuracy of the sensor.

Protein-spiked urine solutions. A 0.1% HSA/PBS solution was spiked in increasing quantities into normoalbuminuric urine from the Stanford Diabetes Clinic and diluted in PBS 10-fold (up to 149 µL total volume) to create urine solutions with protein concentrations spanning from 0.0013

175 g/dL to 0.86 g/dL. After testing a number of different dilutions, we found that 10-fold dilution
176 optimally minimized background interference from the urine matrix while still maintaining good
177 sensitivity for protein analysis. One microliter of Cy5.5 dye solution was added to each tube with
178 mixing, and the samples were then tested with the VCSEL biosensor to obtain a standard curve
179 for urine protein.
180
181 ***Clinical urine samples.*** An initial set of urine samples (n=5) were obtained from patients at the
182 Stanford Diabetes Clinic in accordance with and permission from the Stanford Institutional
183 Review Board (IRB). Patients were instructed to urinate into a plastic urine collection cup, which
184 was immediately sealed and stored on ice, and either tested within 1-2 hours or transferred to 15
185 mL tubes and stored frozen at -20 C for future testing. Additional urine samples (n=9) from
186 diabetic patients that had already been pre-tested by dipstick were purchased from an outside
187 vendor (Lee Biosolutions, Maryland Heights, MO). We first tested (or re-tested) all urine
188 samples by dipstick, and protein content was assessed semi-quantitatively (normal, trace, 1+, 2+,
189 3+, 4+) against color codes provided on the package label. We then tested urine samples for total
190 protein using the VCSEL biosensor and by benchtop fluorimetry. Urine samples also underwent
191 microalbumin testing at the Stanford Clinical Laboratory using gold standard
192 immunonephelometry on a Dimension Vista (Siemens AG, Munich, Germany) chemistry
193 analyzer. Sensor values were plotted against clinical lab values to assess the accuracy of the
194 sensor.
195
196 ***Spectrophotometer measurements.*** Samples and calibration standards (149 uL sample/standard
197 + 1 μL dye) were pipetted in triplicate into a 96-well black microtiter plate, which was read by a

198 Synergy 4 benchtop microplate reader (BioTek, Winooski, VT). The reader was set to
199 fluorescence mode with 675 nm excitation and 710 nm emission. Readings were acquired at
200 room temperature with a 1-second acquisition time per sample. The triplicate fluorescence
201 intensities for each sample and calibration standard were averaged and background subtracted by
202 the average intensity of the negative control samples (buffer + dye) to obtain the net fluorescence
203 signal. Sample concentrations were interpolated from the best-fit curve for the calibration
204 standard intensities.
205
206 ***VCSEL biosensor measurements.*** The excitation VCSELs acquired from Vixar (Plymouth, MN)
207 were current-driven with a sinusoidal 1.5 mA (peak-to-peak), 23Hz waveform, on top of a 10
208 mA DC offset (Keithley Instruments 6221, Cleveland, OH) resulting in an average optical output
209 power of ~0.75 mW at 675 nm at room temperature with narrow laser line widths, minimizing
210 scattered excitation interference. The GaAs detectors exhibit dark currents less than 5 pA/mm^2
211 for 100 mV bias and quantum efficiencies surpassing 75%. The detector output was read out
212 with a lock-in amplifier (Stanford Research Systems SRS 830, Sunnyvale, CA) with a time
213 constant of 30 ms and sensitivity of 20 mV. The instruments were automatically controlled by a
214 MatLab (Mathworks, Natick, MA) program over GPIB interface. With the sensor switched on,
215 150 µL of either sample or standard solution, premixed with Cy5.5 dye, was pipetted into the
216 300 µL sample well. Output data was recorded from the lock-in amplifier in real-time as
217 magnitude of the photocurrent signal at the modulated frequency.
218
219 ***Sensor response time.*** To test the response time of the sensor, fluorescence intensity was
220 recorded as a function of time with addition of dye or protein to buffer in the sensor sample well.

Specifically, a 130 μL volume of PBS was transferred to the sample well and 1 μL of Cy5.5 dye solution was added at 20s. A buffer solution containing 1% HSA and 1% IgG was then added at 30s, and a buffer solution containing 10% HSA and 10% IgG was added at 40s. Time to stabilization of the fluorescence signal change after each of these additions was recorded.

Fluorescence imaging. A microtiter plate containing the samples used for spectrophotometry measurements were positioned within an IVIS Spectrum in vivo imaging system (Perkin Elmer, Waltham, MA) and fluorescence images were acquired with the following settings: 675 nm filter; exposure time: 2s; binning: medium; f-stop: 2. Average radiance was measured by drawing a region of interest (ROI) around each sample well in the acquired image and subtracting the control (buffer and dye only) signal.

Data analysis. GraphPad Prism 5 was used for plotting and statistical analysis**.** All data presented in this paper represent the mean ± standard deviation (SD) of triplicate samples (n=3). Sample and calibration standard fluorescence intensities were background subtracted by control samples to obtain net fluorescence signals. Best-fit standard curves were obtained by linear regression using the calibration standard fluorescence intensities and R^2 correlation coefficients were calculated. Coefficients of variation (CV) were calculated according to: $\boldsymbol{CV} = (SD/Mean) \times 100$. Limit of detection (LOD) and limit of quantification (LOQ) values were calculated using the following: $\boldsymbol{LOD} = \frac{3 \times SD}{s}$ and $\boldsymbol{LOQ} = \frac{10 \times SD}{s}$, as per the International Conference on Harmonisation (ICH) and United States Pharmacopoeia (USP)[35] , where *s* is the slope of response curve. For accuracy measurements, the correlation between sensor and gold

243 standard measurements was assessed using a Pearson R-value and two-tailed P-value
244 ($P<0.0001$).
245

Results and Discussion

Protein Analysis of Spiked Buffer and Pooled Serum Samples. For the 150 µL assay volumes used in our sensor experiments, preliminary results with different amounts of dye and protein showed that 1 µg of Cy5.5 dye was sufficient to detect a wide range of protein concentrations in diluted urine and serum (data not shown). We first characterized the response rate and stability of the sensor signal with introduction of protein to the sample well. Here, protein solutions of increasing concentration were directly added to the existing dye solution to record the time response, instead of premixing as was done in subsequent experiments. As shown in **Fig. 3a**, the sensor responds in < 1 s to introduction of 1 µl of dye to buffer (phosphate buffer saline or PBS), and demonstrates a similarly rapid response or signal increase to subsequent additions of proteins (1% and 10% solutions of human serum albumin (HSA) and immunoglobin G (IgG) in buffer). Addition of the 10% protein mixture may have saturated the signal, hence yielding an increase that is not exactly proportionate relative to the 1% protein mixture, but nevertheless demonstrates the rapid response in detecting the change in protein concentration. Further, the signal is stable over the 2-minute duration of the measurement, attesting to the robustness of the electronic components, the slow off-rate of the protein-dye complex, and minimal photobleaching of the dye.[46] Furthermore, measurements of various serum dilutions on a Synergy 4 benchtop microplate reader (BioTek, Winooski, VT) at 1-minute intervals confirmed negligible degradation of assay signal, even after 10 minutes (**Fig. S1**).

Next, we evaluated the limit of detection (LOD) and dynamic range of the device on buffer spiked with known quantities of purified proteins and on pooled serum. In so doing, our goal was to assess device performance under ideal conditions (spiked buffer) with pure forms of the predominant proteins found in proteinuric urine - human serum albumin (HSA) and

immunoglobulin G (IgG) - as well as in a complex matrix (serum) containing numerous types of proteins and potential small molecule interferents. Incremental amounts of a protein cocktail (5:3.5 ratio of 1%HSA:1%IgG) were spiked into PBS to 149 µL total volume and 1µL of Cy5.5 dye (1mg/mL) was then added and mixed into each sample well. The resulting calibration curve (**Fig. 3b)** demonstrates that the sensor signal is linearly correlated with protein concentration over the range of 0.0027 – 0.34 g/dL, with a correlation coefficient (R^2) of 0.9996. The LOD was 0.0073 g/dL, such that as little as 10 µg of protein could reliably be detected. Similarly, pooled serum was spiked into PBS in incremental volumes (starting from 0.5µL serum spiked into 148.5 µL PBS) to create solutions with a wide range of protein concentrations (0.003 - 0.41 g/dL)(**Fig. S3**). For serum, the calibration curve was linear over a wide range: 0.003-0.22 g/dL (R^2 = 0.9898)(**Fig. 3c**), allowing measurements spanning from well below to well above the normal reference range of serum protein concentrations (6-8.3 g/dL[34], before ~100-fold sample dilution). Furthermore, the slopes of the calibration curves in buffer (Fig 3b.) and serum (Fig. 3c) were close, indicating that the serum matrix does not introduce significant interference on the protein detection as compared to the buffer.

The calibration curve for protein-spiked buffer was then used to interpolate the concentration of the serum dilutions from their sensor signals. These interpolated concentrations were compared against the actual sample protein concentrations as determined by BCA protein analysis, which yielded an accuracy curve with a strong correlation coefficient (R^2=0.99), a y-intercept close to zero, and a slope close to unity (~0.94) (**Fig. 3d**). The average intra-assay coefficient of variation (CV) (n=3) was 5.66%. These results demonstrated that an HSA/IgG-spiked buffer system could be used to accurately calibrate serum protein concentrations, despite the diversity of small molecules, ions, proteins and other potential interferents present in serum.

Performance Comparison of Sensor and Benchtop Spectrophotometer. We compared the performance of the sensor with that of a benchtop microplate reader (e.g. standard fluorimetry) for both serum and urine by running calibration standards on both devices (details of preparing urine calibration standards are provided in the next section). Because the microplate reader's output is given in fluorescence intensity units whereas our sensor's output is in amperes, we normalized both sets of measurements and plotted them for comparison. For serum, the sensor response curve appears to be left-shifted compared with that of the spectrophotometer (**Fig. 4a**). Interestingly, at low concentrations (0.003-0.08 g/dL range), the sensor's dose response is steeper than that of the spectrophotometer. However, the sensor's signal also begins to saturate at lower concentrations compared with the reader, which is likely attributable to the smaller surface area of the sensor's photodiode compared with the reader's photodetector. This saturation can be mitigated by using a higher voltage limit PIN detector, or by placing a more attenuating filter in the optical path, though the latter option will decrease sensitivity. Alternatively, samples that fall within the saturation range can be diluted further so that their concentrations fall within the linear range. We found that serum and urine data had different-shaped best-fit curves (**Fig. S4**), which may be due to their different constituents and calibration matrices. For urine, the best-fit curves for the sensor and spectrophotometer correlated well each other (p-value <0.001, Pearson coefficient r=0.82). (**Fig. 4b**). However, we observed that signal correlated more strongly with protein concentration in the sensor (R^2=0.94) than in the spectrophotometer (R^2=0.69).

VCSEL Sensor Protein Analysis on Clinical Urine Samples. We then proceeded to test the device on urine samples from patients with type II diabetes (n=14). A calibration curve was

obtained by spiking two-fold serial additions of HSA (0.1% stock) into a normoalbuminuric urine sample (**Fig. 5a**), and the resulting spiked urine samples were further diluted 10-fold to ensure that protein concentrations were within the linear range of the assay and to minimize the contribution of interferents. While a logarithmic dose response could be used to fit the calibration data (R^2=0.91), a better fit was obtained with a bilinear curve: a steep line at very low protein concentrations (0.0013-0.021 g/dL), with a slope of 35.95 (R^2=0.997) and a shallower line at intermediate to high concentrations (0.043-0.86 g/dL) with a slope of 1.52 (R^2=0.988). The bilinear response could be attributed to limitations in the sensor's dynamic reserve, resulting in lower resolution at higher concentrations and hence a flatter slope. The limits of detection and quantitation were 0.0004 g/dL and 0.0013 g/dL, respectively, using established calculation methods[35]. The sensor's dynamic range (0.0013-0.86 g/dL) covers the range of urine protein concentrations seen in microalbuminuria (0.02-0.20 g/dL)[41], and in fact spans a wide range of dipstick protein concentrations from trace to 3+ (0.0050-0.15 g/dL)[42].

There are no definitive guidelines as to whether proteinuria should be defined in terms of albumin or total protein loss[36]. Although urine total protein is the strongest predictor of adverse outcomes in chronic kidney disease, urine albumin is the more commonly used biomarker for early diabetic nephropathy. Therefore, our next goal was to assess whether our sensor's urine total protein measurements would be a reliable surrogate for urine albumin in diabetics. We tested our clinical urine samples (n=14) with the sensor and used the calibration curve obtained above (**Fig. 5a)** to interpolate the sample protein concentrations (**Fig. 5b, c**). The average intra-assay CV (n=3) within the working range of the assay was 21.5%. However, without the two samples that had a large quantity of sediment, the intra-assay CV (n=3) was 13.9%. For each sample, we then plotted the sensor-derived total protein value against the albumin concentration,

as determined by gold standard immunonephelometry (**Figs. 5d, e**). We found that urine total protein was strongly correlated with urine albumin across a wide range of urine albumin levels seen clinically (p-value <0.0001, Pearson r = 0.957). Sensor measurements of total protein correlated strongly with gold standard nephelometric measurements of albumin in the low concentration regime (0-0.05 g/dL, R^2 = 0.989), and only somewhat less so in the high concentration regime (>0.05 g/dL, R^2= 0.857). Even within the high concentration regime, the linear correlation is qualitatively quite strong up to ~0.15 g/dL, and falls off afterwards. This could potentially be attributed to: (1) the presence of sediments that were observed in the two urine samples with the highest protein concentrations, causing interference; (2) poor correlation between urine total protein and urine albumin at high concentrations, possibly due to the presence of other interfering urinary proteins that can pass through a compromised glomerular basement membrane (IgG, myoglobin); or (3) lower sensor accuracy at higher urine protein concentrations. To address (1), we could filter out urinary sediment in future studies and redesign our sensor to contain microfluidic pre-filtration steps to clear the urine of sediment prior to reaction with dye. To address (2) and (3), urine sample could be measured at a few different dilutions to ensure that even high protein samples fall within the linear range of our assay. In addition, (3) could be addressed by increasing the dynamic reserve of the lock-in amplifier. Nevertheless, the high correlation between urine protein and urine albumin at concentrations <0.05 g/dL suggests that these two markers are interchangeable at low concentrations, and that our total protein assay is a reliable surrogate for albumin in detecting microalbuminuria.

Overall, the VCSEL biosensor has several advantages over current clinical protein quantitation methods and fluorimeters in terms of size, speed, sensitivity, cost, and sample requirement (**Table S1**). The miniaturization and the on-chip integration of all components

within a 9 mm footprint make our device portable and suitable for point-of-care use.

Compared to turbidimetric and nephelometric immunoassays for albumin, or colorimetric assays for total protein, our assay is a simple and rapid two-component reaction that requires only 1-2 seconds of mixing and no washing, incubation, or heating steps. Because the PIFE fluorescence change is nearly instantaneous (<1 second) and proportional to sample protein concentration, the device can effectively measure total protein in real time, making it ideal for point-of-care and frequent monitoring applications like sudden drops in serum protein levels, as can occur in sepsis or after major surgery[45].

While the urine volumes used by the VCSEL biosensor (10-20 µL) are comparable to those used for clinical measurements of albumin and total protein in clinical chemistry analyzers, the plasma or serum volume required is only 1.5 µL. The low volume requirement is ideal for point-of-care testing, allowing serum total protein to be measured from as little as a finger prick of blood (~5-10 µL).

The cost of goods for the VCSEL biosensor is orders of magnitude lower than that of commercial benchtop fluorimeters (~$2,000 for Qubit fluorimeter) and small microplate readers (>$5,000), not to mention large clinical chemistry analyzers (>$30,000). When purchased in bulk, the costs of VCSELs, PIN detectors, and collimating lenses are $2-4, $0.10-0.50, and $3-4, respectively. Additional costs for a standalone device include firmware with Bluetooth (~$10-20), diode amplifier (~$10), battery ($1-2), and sample well ~$0.02. Thus, the estimated cost of the entire sensing platform is ~$30. Also, unlike immunoturbidimetry, which requires the expense of antibodies, our assay requires minimal quantities of an inexpensive reagent, Cy5.5 fluorescent dye ($0.10 per test), and readily available buffers. The cost-effectiveness of the device can enable broad screening for microalbuminuria in patients with diabetes and healthy

persons, allowing for early-stage intervention with anti-hypertensive treatment, which can stabilize or slow the progression of renal disease[38].

The VCSEL biosensor's limit of detection is 5-10 fold better than the gold standard pyrogallol method used in clinical labs for total protein analysis. The sensor can detect as little as 1.95 µg of total protein (0.013 µg/µL LOQ× 150 µL well volume), compared to 21.6 µg of total protein detectable by the gold standard Pyrogallol method[43] (**Table S1**).

Conclusion

According to the CDC, an estimated ~96% of people with kidney damage (e.g., mildly reduced kidney function) are unaware of it. Therefore, the ability to monitor urine albumin and protein levels routinely outside the doctors' office would likely improve surveillance and screening of kidney disease in patients with diabetes and the general population, and empower individuals to track their own health. The use of urine total protein as a surrogate marker for urine albumin has been previously proposed[10-13], and has the advantage of being measurable with dye-based reagents, which afford faster and less expensive assays. However, existing fluorescence detection instruments, including benchtop fluorimeters, microplate readers, and chemistry analyzers for *in vitro* analyses are bulky and expensive and do not permit portable, in-home, real-time urine protein analysis. Therefore, new methods are needed to easily and accurately monitor renal health on a routine basis both in patients with diabetes and in the general population.

We have developed a miniaturized VCSEL biosensor for PIFE-based measurement of total protein in human urine and serum, with applications in point-of-care and routine home monitoring of renal health. The discretely integrated device consists of a 675-nm VCSEL laser excitation source, a PIN photodiode, an optical filter, and a collimating lens, all within a package

of 9-mm footprint. The device sits directly beneath a sample well, where a 150 µl volume of a pre-diluted biofluid sample is mixed with Cy5.5 dye, yielding an instantaneous and measurable fluorescence enhancement in proportion to protein concentration (PIFE phenomenon). This is the first study that we know of demonstrating the design and implementation of a VCSEL-based sensor for urine and serum total protein measurements and for real-time bio-analyte sensing.

We tested the device on pooled human serum from healthy individuals and urine from patients with diabetes and demonstrated that our easy-to-use platform achieves sensitive (1.95 µg protein limit of detection) and accurate real-time total protein measurements over a wide dynamic range (>2 orders of magnitude) using minimal sample volumes (<15 µL). Calibration curves using serum-spiked buffer and HSA-spiked urine were linear across a wide range of physiologically-relevant protein concentrations. Coupled with its low detection limit, the sensor's high dose response in the low protein concentration range could make it a powerful screening tool since small changes in urine protein concentration within the "normal" range are magnified in a quantifiable way, thus providing the potential to better alert an otherwise healthy individual of early kidney disease and progression.

While we demonstrate the VCSEL sensor's use for plasma and urine protein measurement, the technology could be further extended to other biofluids, including saliva, sweat, tears, or cerebrospinal fluid. Other potential medical applications of the device include home monitoring of urine protein for rapidly progressive glomerulonephritis and surveillance for kidney transplant rejection, and monitoring of serum protein levels in liver disease. In addition, our sensor and PIFE protein assay are not limited to use with Cy5.5, and can be used with other dyes and for other optical assay applications as described further in the supplemental section. Furthermore, the device could be extended to include an array of VCSELs with different

excitation wavelengths along with their corresponding optical filters and detectors to detect multiple analytes, enabling on-chip multiplexed sensing. Our platform thus holds great promise for personalized and mobile health monitoring.

Acknowledgments. We would like to acknowledge the Stanford Clinical Laboratory for running our clinical samples, the Canary Center at Stanford for Cancer Early Detection, James Strommer for help with figure design, and Dr. Carmel Chan for helpful suggestions and comments. Funding: This research was supported by a grant from the Canary Foundation.

Author contributions: FM, OV, JL, SSG, and JH conceived of the project idea. FM designed the sensor customized for in-vitro sampling of small liquid volumes. OV inspired the idea of using a PIFE-based assay for total protein analysis. FM and OV performed the experiments, analyzed the data, and wrote the manuscript. JL advised on the chemistry aspects of the experiments. MT provided guidance and patient samples for the clinical study. ISA helped with IVIS experiments and BCA protein measurements. JH, SSG, and OV supervised the project. All authors discussed the results and contributed to the final manuscript. Competing interests: The authors have no competing interests or other interests that might be perceived to influence the results and/or discussion reported in this article. Data and materials availability: All data associated with this study are available in the main text or the supplementary materials.

Additional information. Patient samples were collected in accordance with and permission from Stanford Institutional Review Board (IRB) from Stanford Diabetes Clinic.

References

1. American Diabetes Association. “Standards of Medical Care in Diabetes-2013.” *Diabetes Care*, American Diabetes Association, 1 Jan. 2013. care.diabetesjournals.org/content/36/Supplement 1/S11.

2. Center for Disease Control & Prevention. “National diabetes statistics report: estimates of diabetes and its burden in the United States”, 2014. Atlanta, GA: US Department of Health and Human Services 2014.

3. Zeeuw, D. De. “Albuminuria, Just a Marker for Cardiovascular Disease, Or Is It More?” *Journal of the American Society of Nephrology*, vol. 16, no. 7, 2005, pp. 1883–1885. doi:10.1681/asn.2005050524.

4. Jong, P. E. De. “Screening, Monitoring, and Treatment of Albuminuria: Public Health Perspectives.” *Journal of the American Society of Nephrology*, vol. 17, no. 8, 2006, pp. 2120–2126., doi:10.1681/asn.2006010097.

5. “KDOQI Clinical Practice Guidelines and Clinical Practice Recommendations for Diabetes and Chronic Kidney Disease.” *American Journal of Kidney Diseases*, vol. 49, no. 2, 2007, doi:10.1053/j.ajkd.2006.12.005.

6. Martin, Helen. “Laboratory Measurement of Urine Albumin and Urine Total Protein in Screening for Proteinuria in Chronic Kidney Disease.” *The Clinical Biochemist Reviews* 32.2 (2011): 97–102.

7. Comper, Wayne D., et al. “High Prevalence of Immuno-Unreactive Intact Albumin in Urine of Diabetic Patients.” *American Journal of Kidney Diseases*, vol. 41, no. 2, 2003, pp. 336–342., doi:10.1053/ajkd.2003. 50041.

8. Incerti, Juliane, et al. “Evaluation of Tests for Microalbuminuria Screening in Patients with Diabetes.” *Nephrology Dialysis Transplantation*, vol. 20, no. 11, 2005, pp. 2402–2407., doi:10.1093/ndt/gfi074.

9. Pavlovic, Drasko, Laboratory Standards in the Diagnosis and Monitoring of Therapy - eJIFCC 20/01 2009 http://www.ifcc.org

10. Hashemipour, Sima, et al. “Urinary Total Protein as the Predictor of Albuminuria in Diabetic Patients.” *International Journal of Endocrinology & Metabolism*, vol. 10, no. 3, 2012, pp. 523–526., doi:10.5812/ijem.4236.

11. Khatami, Zhara, et al. “Screening For Microalbuminuria By Use Of Microproteinuria.” *East Mediterr Health J*. 2005 May;11(3):358-65.

12. C., Robert, et al. “Association between Albuminuria and Proteinuria in the General Population: the AusDiab Study”, *Nephrology Dialysis Transplantation,OUP Academic*, Oxford University Press, 1 Oct. 2003, academic.oup.com/ndt/article/18/10/2170/1807563

13. Marshall, Thomas, and Katherine M. Williams. “Total Protein Determination in Urine: Elimination of a Differential Response between the Coomassie Blue and Pyrogallol Red Protein

Dye-Binding Assays." *Clinical Chemistry*, Clinical Chemistry, 1 Mar. 2000, clinchem.aaccjnls.org/content/46/3/392.

14. Olson, B J, and J Markwell. "Assays for Determination of Protein Concentration." *Current Protocols in Protein Science.*, U.S. National Library of Medicine, May 2007, www.ncbi.nlm.nih.gov/pubmed/18429326.

15. Smith, P K, et al. "Measurement of Protein Using Bicinchoninic Acid." *Analytical Biochemistry.*, U.S. National Library of Medicine, Oct. 1985, www.ncbi.nlm.nih.gov/pubmed/3843705.

16. LOWRY, O H, et al. "Protein Measurement with the Folin Phenol Reagent." *The Journal of Biological Chemistry.*, U.S. National Library of Medicine, Nov. 1951, www.ncbi.nlm.nih.gov/pubmed/14907713.

17. Carroll, Michael F., and Jonathan L. Temte. "Proteinuria in Adults: A Diagnostic Approach." *AAFP Home*, 15 Sept. 2000, www.aafp.org/afp/2000/0915/p1333.html.

18. Yılmaz, Fatma Meriç, et al. "Automated Turbidimetric Benzalkonium Chloride Method for Measurement of Protein in Urine and Cerebrospinal Fluid." *Clinical Chemistry*, Clinical Chemistry, 1 Aug. 2004, clinchem.aaccjnls.org/content/50/8/1450.

19. Iga, K. "Surface-Emitting Laser-Its Birth and Generation of New Optoelectronics Field." *IEEE Journal of Selected Topics in Quantum Electronics*, vol. 6, no. 6, 2000, pp. 1201–1215., doi:10.1109/2944.902168.

20. Hibbs-Brenner, M. K., et al. "VCSEL Technology for Medical Diagnostics and Therapeutics." *Photons and Neurons*, 2009, doi:10.1117/12.815307.

21. Mateus, C.f.r., et al. "Compact Label-Free Biosensor Using VCSEL-Based Measurement System." *IEEE Photonics Technology Letters*, vol. 16, no. 7, 2004, pp. 1712–1714., doi:10.1109/lpt.2004.828851.

22. Mateus, C.f.r., et al. "Ultra Sensitive and Compact VCSEL-Based Biosensor for Detection of Protein Interactions and Dengue Antibodies." *Digest of the LEOS Summer Topical Meetings Biophotonics/Optical Interconnects and VLSI Photonics/WBM Microcavities*, 2004, doi: 10.1109/leosst.2004.1338664.

23. Nakazato, K. "Chemistry Integrated Circuit: Chemical System on a Complementary Metal Oxide Semiconductor Integrated Circuit." *Philosophical Transactions of the Royal Society A: Mathematical, Physical and Engineering Sciences*, vol. 372, no. 2012, 2014, pp. 20130109–20130109, doi: 10.1098/rsta.2013.0109.

24. O'Sullivan,T., et al. "Implantable semiconductor biosensor for continuous in vivo sensing of far-red fluorescent molecules." *Opt. Express 18*, 12513-12525, 2010, vol 18, no.12, pp 12513-12525, **https://doi.org/10.1364/OE.18.012513**

25. Sullivan, T., "Implantable Fluorescence Sensor For Continuous Molecular Monitoring In Live Animals", *Ph.D. Dissertation, Dept. Elect. Eng., Stanford Univ.*, Stanford, CA, 2010.

26. Stennett, Elana M. S., et al. “Demystifying PIFE: The Photophysics Behind the Protein-Induced Fluorescence Enhancement Phenomenon in Cy3.” *The Journal of Physical Chemistry Letters*, vol. 6, no. 10, 2015, pp. 1819–1823., doi:10.1021/acs.jpclett.5b00613.

27. Stennett, Elana M. S., et al. “Photophysical Processes in Single Molecule Organic Fluorescent Probes.” *Chem. Soc. Rev.*, vol. 43, no. 4, 2014, pp. 1057–1075., doi:10.1039/c3cs60211g.

28. Sanborn, Matthew E., et al. “Fluorescence Properties and Photophysics of the Sulfoindocyanine Cy3 Linked Covalently to DNA.” *The Journal of Physical Chemistry B*, vol. 111, no. 37, 2007, pp. 11064–11074., doi:10.1021/jp072912u.

29. Hwang, Helen, and Sua Myong. “Protein Induced Fluorescence Enhancement (PIFE) for Probing Protein–Nucleic Acid Interactions.” *Chem. Soc. Rev.*, vol. 43, no. 4, 2014, pp. 1221–1229., doi:10.1039/c3cs60201j.

30. Luo, G., et al. “Single-Molecule and Ensemble Fluorescence Assays for a Functionally Important Conformational Change in T7 DNA Polymerase.” *Proceedings of the National Academy of Sciences*, vol. 104, no. 31, 2007, pp. 12610–12615., doi:10.1073/pnas.0700920104.

31. Maxwell, Brian A., and Zucai Suo. “Single-Molecule Investigation of Substrate Binding Kinetics and Protein Conformational Dynamics of a B-Family Replicative DNA Polymerase.” *Journal of Biological Chemistry*, vol. 288, no. 16, 2013, pp. 11590–11600., doi:10.1074/jbc.m113.459982.

32. König, Sebastian L.b., et al. “Helicase-Mediated Changes in RNA Structure at the Single-Molecule Level.” *RNA Biology*, vol. 10, no. 1, 2013, pp. 133–148., doi:10.4161/rna.23507.

33. Aramendia, Pedro F., et al. “Temperature Dependence of Fluorescence and Photoisomerization in Symmetric Carbocyanines.Influence of Medium Viscosity and Molecular Structure.” *The Journal of Physical Chemistry*, vol. 98, no. 12, 1994, pp. 3165–3173., doi:10.1021/j100063a020.

34. “Total Protein: MedlinePlus Medical Encyclopedia.” *MedlinePlus*, U.S. National Library of Medicine, medlineplus.gov/ency/article/003483.htm.

35. Shrivastava, Alankar, and Vipinb Gupta. “Methods for the Determination of Limit of Detection and Limit of Quantitation of the Analytical Methods.” *Chronicles of Young Scientists*, vol. 2, no. 1, 2011, p. 21., doi:10.4103/2229-5186.79345.

36. Lamb, E. J, et al. “How Should Proteinuria Be Detected and Measured?” *Annals of Clinical Biochemistry*, vol. 46, no. 3, 2009, pp. 205–217., doi:10.1258/acb.2009.009007.

37. Hillege, H. L., et al. “Microalbuminuria Is Common, Also in a Nondiabetic, Nonhypertensive Population, and an Independent Indicator of Cardiovascular Risk Factors and Cardiovascular Morbidity.” *Journal of Internal Medicine*, vol. 249, no. 6, 2001, pp. 519–526., doi:10.1046/j.1365-2796.2001.00833.x.

38. Romundstad, Solfrid, et al. “Microalbuminuria and All-Cause Mortality in 2,089 Apparently Healthy Individuals: a 4.4-Year Follow-up Study. The Nord-Trøndelag Health Study (HUNT), Norway.” *American Journal of Kidney Diseases*, vol. 42, no. 3, 2003, pp. 466–473., doi:10.1016/s0272-6386(03)00742-x.

39. Klausen, Klaus, et al. "Very Low Levels of Microalbuminuria Are Associated With Increased Risk of Coronary Heart Disease and Death Independently of Renal Function, Hypertension, and Diabetes." *Circulation*, vol. 110, no. 1, 2004, pp. 32–35., doi:10.1161/01.cir.0000133312.96477.48.

40. Center for Disease Control & Prevention. "National Chronic Kidney Disease Factsheet, 2017", 2017. Atlanta, GA: US Department of Health and Human Services 2017.

41. Bennett, Peter H., et al. "Screening and Management of Microalbuminuria in Patients with Diabetes Mellitus: Recommendations to the Scientific Advisory Board of the Nationals Kidney Foundation from an Ad Hoc Committee of the Council on Diabetes Mel of the National Kidney Foundation." *American Journal of Kidney Diseases*, vol. 25, no. 1, 1995, pp. 107–112., doi:10.1016/0272-6386(95)90636-3.

42. Kallen, Ronald J., Arnold, Watson C., "Proteinuria", *eMedicine*, 2008, http://emedicine.medscape.com/article/984289-overview

43. Siemens, "Dimension clinical chemistry system-Flex reagent cartridge: UCFP", Product Insert 2015.

44. "Total Protein Test: Purpose, Procedure & Results." *Healthline*, Healthline Media, www.healthline.com/health/total-protein#results.

45. Valuchova, Sona, et al. "A Rapid Method for Detecting Protein-Nucleic Acid Interactions by Protein Induced Fluorescence Enhancement." *Scientific Reports*, vol. 6, no. 1, 2016, doi:10.1038/srep39653.

46. Ha, Taekjip and Philip Tinnefeld. "Photophysics of fluorescent probes for single-molecule biophysics and super-resolution imaging" *Annual review of physical chemistry* vol. 63 (2012): 595-617.

631 **Figures**

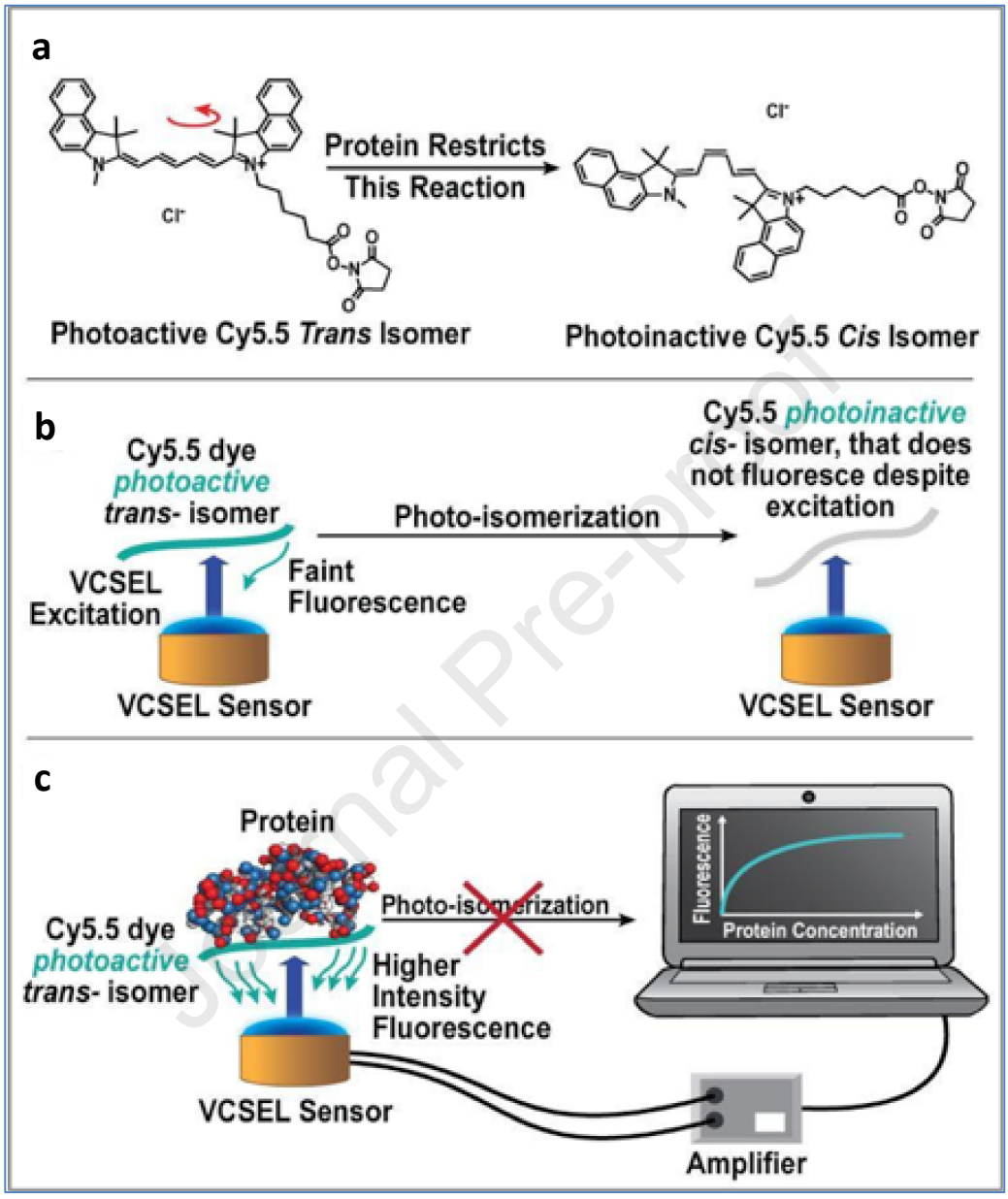

632

633 **Fig. 1 Protein-induced fluorescence enhancement of Cy5.5 dye. a.** Schematic of Cy5.5
634 photoisomerization between the photoactive *trans* isomer and the photoinactive *cis* isomer. **b.**
635 Lower intensity fluorescence in absence of protein: Cy5.5 dye exists as a photoactive *trans*
636 isomer at ground state that fluoresces upon excitation and tends to undergo photo-isomerization,
637 converting to a fluorescently inactive *cis* isomer **c.** Higher intensity fluorescence in the presence
638 of protein: when a protein is present in the vicinity of the dye, it sterically hinders isomerization
639 and stabilizes the *trans* conformation in the photoactive state, resulting in a higher fluorescence
640 quantum yield and a longer excited-state lifetime. As the VCSEL laser excites the sample, the
641 emitted fluorescence is captured by an on-chip detector, yielding current in proportion to
642 fluorescence intensity.

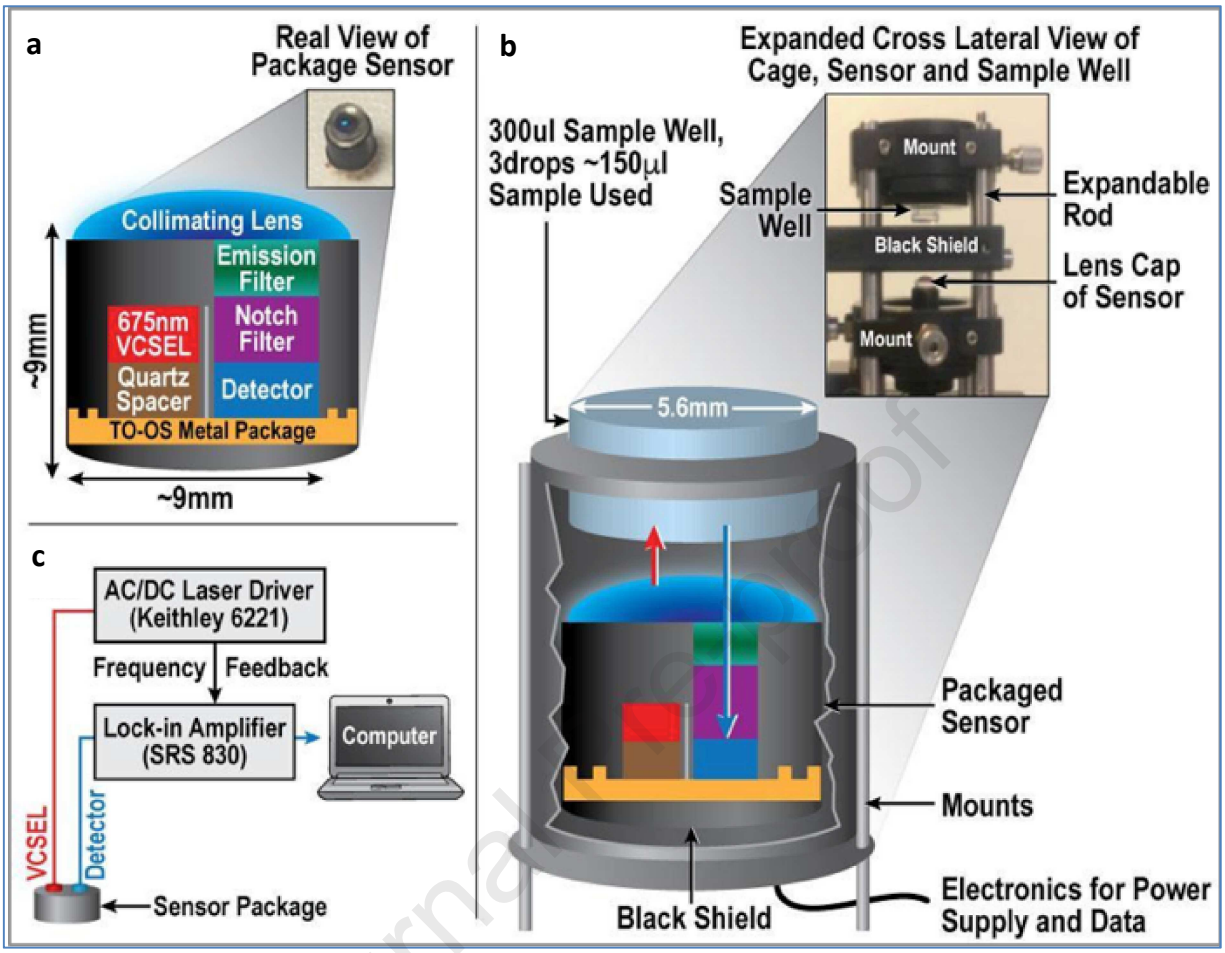

Fig. 2 Biosensor architecture. a. Schematic cross-sectional view of the biosensor showing the VCSEL, PIN detector, and optical filters encased within a TO-5 metal package with a collimating lens. **b.** Schematic of test setup comprising the VCSEL sensor from (a) and a sample well mounted directly above it. Inset: Image showing an exploded view of the setup. **c.** Block diagram of the VCSEL and detector connected to a laser driver, lock-in amplifier, switch, and computer.

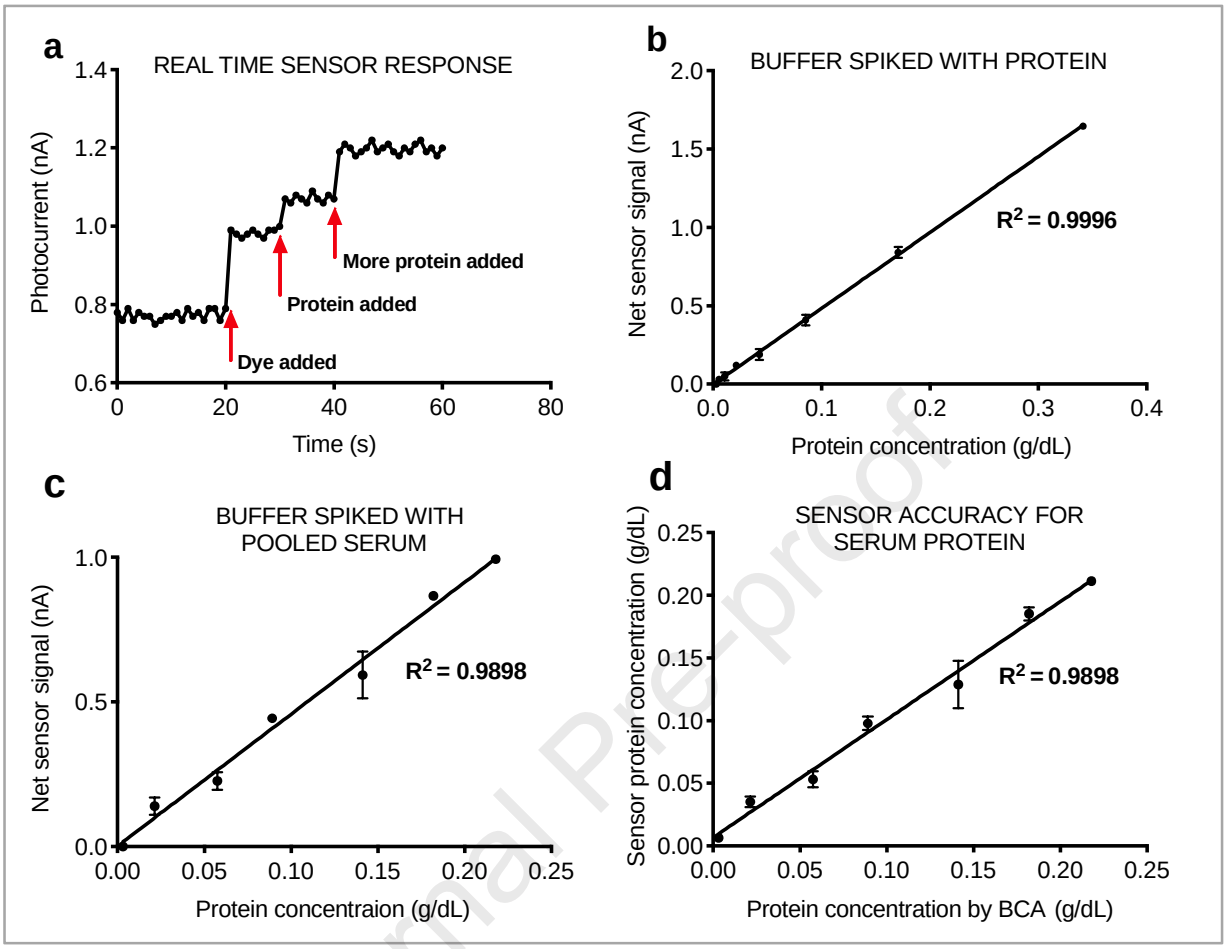

Fig. 3 Sensor response and accuracy. a. The sensor exhibits an instantaneous response and fast equilibration upon addition of Cy5.5 dye to buffer at 20s, followed by 4 µL additions of 1% and 10% human serum albumin (HSA)+immunoglobin G (IgG) solutions at 30s and 40s, respectively. The signal changes are relatively stable over the intervals shown. **b.** Calibration curve showing strong correlation of sensor response with protein concentration in HSA/IgG-spiked buffer over the linear range (~0.003-0.34 g/dL). Best-fit line: y = 4.845x – 0.0008. Error bars represent standard deviations (s.d.); however, some are too small to be visible on the scale of the graph. **c.** Calibration curve showing the strong correlation of sensor response with quantity of serum spiked into buffer solution over the linear range (0.003-0.2179 g/dL protein). Best-fit line: y = 4.558x + 0.0023. Protein concentrations for the various serum dilutions were determined by BCA protein analysis. **d.** Biosensor accuracy for measuring protein concentrations in serum. The calibration curve for protein-spiked buffer in (b) was used to interpolate the protein concentrations of the various serum dilutions in (c). These interpolated values were plotted in (d) against the actual protein concentrations as determined by BCA protein analysis to demonstrate the accuracy of our method. Best-fit line: y = 0.9407x + 0.0068 (n=3 replicates for each data point, mean ± s.d.).

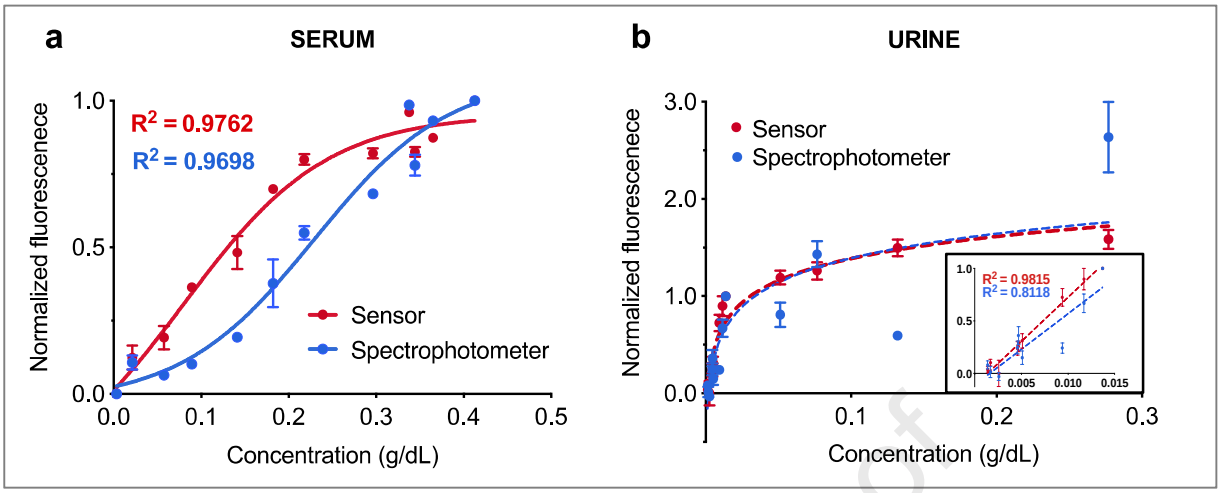

Fig. 4 Comparison of Sensor Performance with Benchtop Spectrophotometer. Sensor and microplate reader measurements for **a**. serum dilutions in buffer, and **b.** spiked urine samples after 10-fold dilution. For urine, the sensor best-fit curve is: y = 0.33ln(x) – 0.87; the spectrophotometer best-fit curve is: y = 0.36ln(x) – 1.10. Inset shows best fit curves for pre-saturation urine protein concentrations. For serum and urine, measurements were normalized to the maximum linear (pre-saturation) signal (n=3 replicates for each data point, mean ± s.d.).

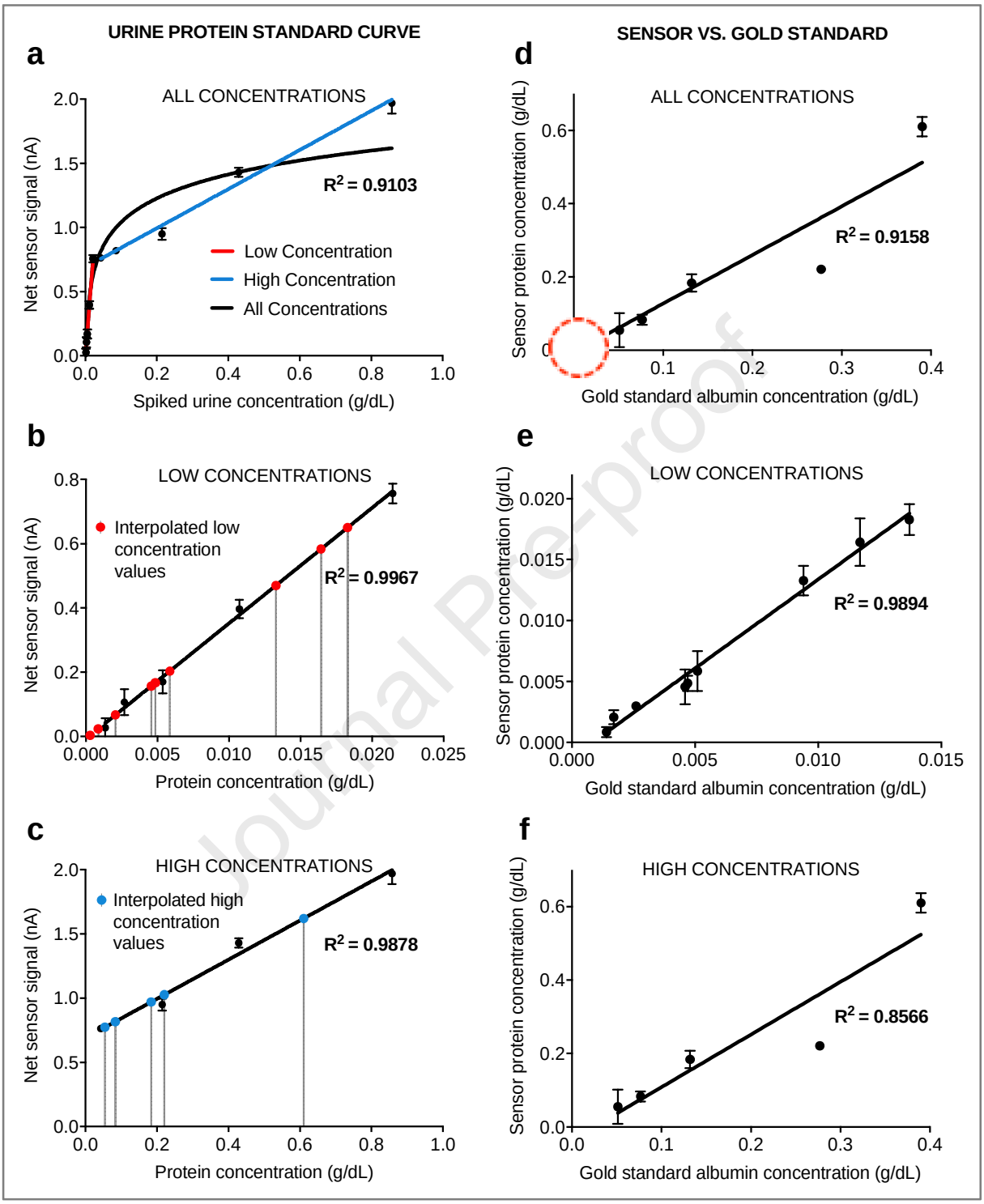

Fig. 5 Sensor Calibration Curve and Comparison with Gold Standard. a. Calibration curve showing sensor response versus urine protein concentration (0.0013-0.86 g/dL) for HSA-spiked human urine (error bars = s.d.). A two-part curve (blue and red lines) provides a better fit to the data than a logarithmic curve (black)(n=10 concentrations, n=3 replicates each, mean ± s.d).

b. Clinical urine samples with sensor signal < 0.8 nA were interpolated over the calibration curve's low range (0.0013-0.021g/dL), corresponding to the red line in (a). The sensor shows particularly high dose response (e.g. large change in signal for small change in protein concentration) over this low concentration range. Best-fit line: $y = 35.95x - 0.0074$. **c.** Clinical urine samples with sensor signal > 0.8nA were interpolated over the calibration curve's high range (0.043-0.858g/dL), corresponding to the blue line in (a). Best-fit line: $y = 1.52x + 0.69$. **d.** Comparison of protein measurements with the sensor versus albumin measurements by gold standard nephelometry for urine samples, establishing accuracy and correlation (n=14 concentrations, n=3 replicates each, mean ± s.d). Best-fit line: $y = 1.33x - 0.0059$. **e.** Zoom-in view of the red dashed circle in (d), showing a high correlation with the gold standard in the lower range of urine protein concentrations. Best-fit line: $y = 1.46x - 0.0012$. **f.** A slightly lower correlation is seen in the higher range of urine protein concentrations. Best-fit line: $y = 1.43x - 0.035$.

Highlights

- VCSEL-based sensor and PIFE assay are combined for miniaturized, real-time urine protein sensing.
- Sensitive and rapid (< 1 second) detection of as little as 1.95 µg protein in a biofluid sample.
- Wide dynamic range spans physiologically-relevant protein concentrations in serum and urine.
- Sensor urine total protein in patients with diabetes strongly correlates with gold standard test.
- High dose response at low protein levels could permit early detection of diabetic nephropathy.
- Low cost, small size, and minimal power requirements can afford portability for mobile health.

Declaration of interests

☒ The authors declare that they have no known competing financial interests or personal relationships that could have appeared to influence the work reported in this paper.

☐The authors declare the following financial interests/personal relationships which may be considered as potential competing interests: